GEOPHYSICAL RESEARCH LETTERS, VOL. 26, NO. 18, PAGES 2845-2848, SEPTEMBER 15, 1999

Analysis of early phase ring current recovery mechanisms during geomagnetic storms

M. W. Liemohn,[1] J. U. Kozyra,[1] V. K. Jordanova,[2] G. V. Khazanov,[3] M. F. Thomsen,[4] and T. E. Cayton[4]

Abstract. A time-dependent kinetic model is used to investigate the relative importance of various mechanisms in the early phase decay rate of the ring current. It is found that, for both the solar maximum storm of June 4-7, 1991 and especially the solar minimum storm of September 24-27, 1998, convective drift loss out the dayside magnetopause is the dominant process in removing ring current particles during the initial recovery. During the 1998 storm, dayside outflow losses outpaced charge exchange losses by a factor of ten.

Introduction

The cause of the rapid decay rate of the ring current during geomagnetic storms is a subject of debate. During storms, the ring current is enhanced, and an indicator of its strength is the *Dst* index, which exhibits a minimum during the main phase of a storm, usually followed by a two-phase decay. Based on AMPTE/CCE observations, *Hamilton et al.* [1988] stated that the faster, early stage recovery from the *Dst* minimum is dominated by the O^+ charge-exchange loss rate and the slower, later stage recovery is governed by the H^+ charge exchange loss rate. *Daglis et al.* [1997] also found observational evidence for this mechanism in CRRES measurements, noticing that the fraction of ring current energy from O^+ drops simultaneously with *Dst*. Recent modeling results, however, have not satisfactorily corroborated this claim, with some stating that it is reasonably adequate in creating this rapid recovery [*Jordanova et al.*, 1996, 1998] and others that it is not [*Fok et al.*, 1995; *Kozyra et al.*, 1998; *Chen et al.*, 1998, 1999]. Additionally, these studies usually examine a single storm, so it is also unclear whether storms at different phases of the solar cycle should exhibit different decay rates because of varying O^+ contributions to the ring current.

Only one study has quantitatively examined losses out the dayside [*Takahashi et al.*, 1990]. They showed that the amount of plasma captured on closed field lines is dependent on both energy and length of recovery for the cross-polar cap potential difference, proposing that the two-phase decay process is from "flow-out" during the rapid recovery phase and charge exchange during the slow recovery phase. That study considered only a few energies, though, with model storm profiles and characteristic loss timescales. In this study, the total energy balance in the entire ring current during two storms (solar minimum and solar maximum) is rigorously modeled and the relative contribution of each source and loss process is examined. The storms of choice are the events of June 4-7, 1991 and September 24-27, 1998. Both involve sudden enhancements in the solar wind pressure striking the magnetosphere. The first storm is during solar maximum, when oxygen content in the stormtime injections is expected to be high, and the second storm is during solar minimum, when the oxygen contribution to the ring current is less.

[1]Space Physics Research Laboratory, University of Michigan, Ann Arbor
[2]Space Science Center, University of New Hampshire, Durham
[3]Geophysical Institute, University of Alaska Fairbanks
[4]Los Alamos National Laboratory, Los Alamos, New Mexico

Paper number 1999GL900611.
0094-8276/99/1999GL900611$05.00

Model description

This study uses the ring current-atmosphere interaction model [*Jordanova et al.*, 1996, 1998] to calculate the phase space distribution function Q for each ring current species. This model solves the bounce-averaged kinetic equation

$$\frac{\partial Q}{\partial t}+\frac{1}{R_0^2}\frac{\partial}{\partial R_0}\left(R_0^2\left\langle\frac{dR_0}{dt}\right\rangle Q\right)+\frac{\partial}{\partial \varphi}\left(\left\langle\frac{d\varphi}{dt}\right\rangle Q\right)+\frac{1}{\sqrt{E}}\frac{\partial}{\partial E}\times\left(\sqrt{E}\left\langle\frac{dE}{dt}\right\rangle Q\right)+\frac{1}{\mu_0 h(\mu_0)}\frac{\partial}{\partial \mu_0}\left(\mu_0 h(\mu_0)\left\langle\frac{d\mu_0}{dt}\right\rangle Q\right)=\left\langle\frac{\delta Q}{\delta t}\right\rangle \quad (1)$$

as a function of position in the magnetic equatorial plane (R_0, φ); velocity variables of energy and equatorial pitch angle (E, μ_0); and time t. In (1), the loss mechanisms included in the right-hand side are charge exchange, Coulomb collisions, and precipitation. Implicitly included in the left-hand side, however, are convective drift gains and losses. This can be separated into a source through the nightside boundary, a loss through the dayside boundary, and a gain or loss due to energy drift within the simulation domain.

Several modifications have been made to the model for this study. First, an analytical description of the magnetopause location as a function of solar wind parameters [*Shue et al.*, 1998] has been included in the model. During extreme solar wind conditions when the magnetopause encroaches on the simulation domain (geosynchronous orbit), the model uses this formulation to define a new outer boundary. Ring current ions beyond this boundary are lost. With this, the model captures the true losses out the dayside magnetopause, especially during the main phase of a storm when the magnetopause will be most compressed.

Secondly, a new injection boundary condition has been developed based on drift path trajectories. These drift paths are dependent not only on the particle's energy but also on the particle's pitch angle, the geomagnetic activity level, and the choice of electric and on magnetic field description. Even the application of satellite data is difficult, because these trajectory differences complicate the extrapolation of point source observations to other locations and times. To handle this complexity, tables have been created specifying the open-closed drift path boundary at geosynchronous orbit as a function of geomagnetic activity, energy, and pitch angle (based on steady-state Volland-Stern drift trajectories). During simulations, these tables are used to determine whether an externally imposed plasma sheet boundary condition or an internally determined boundary condition (determined by using the direction and magnitude of the azimuthal drift at this location to combine the values of neighboring cells) should be applied. This is analogous to the method used for electron injection by *Liemohn et al.* [1998].

Of particular interest for this study are the gains and losses of ring current particles and energy due to convective drift. To examine this, outputs were created to track the particle and energy sources and losses due to every term in (1). Because the code also calculates the total particle and energy count throughout the entire simulation, a comparison of the net gain or loss due to these two methods (flux through the boundaries and entire phase space integration) yields an analysis of the particle and energy conservation of the numerical technique. It was found that slight improvements could be made to the scheme, and the resulting ratio of these two methods for total particle change (ΔN/Δt) and total energy change (ΔE/Δt) is shown in Figure 1 for a typical storm. The particle and energy changes agree remarkably well between the two methods, with the difference usually much less than one percent. Larger differences often coincide with sign changes of the quantity, when the values approach zero.

Results and discussion

Two storms are simulated for this study: the June 1991 event and the September 1998 event. Solar wind and geophysical characteristics of the two events are shown in Figure 2. Both events show a dramatic increase in solar wind density and velocity accompanied by southward interplanetary magnetic field (IMF). June 1991 is far more complex than the relatively clean event of September 1998, but both show a similar trend. The *Kp* histories during these events are also plotted, with both showing a major disturbance with *Kp*>8.

Data from the Los Alamos (LANL) geosynchronous orbit satellite instruments MPA [*McComas et al.*, 1993] and SOPA [*Belian et al.*, 1992] are used for the plasma sheet input values, taken as a time series from measurements obtained within 4 hours of local time around magnetic midnight. Values were averaged when more than one spacecraft was simultaneously in the selection region during a UT interval, and gaps in the data, produced when no satellites were within the near-midnight region, were filled with linear interpolation. These values were then used as a time-dependent boundary condition applied to the entire nightside, but only for open drift path regions determined according to the method described above. Because MPA and SOPA do not measure ion composition, the values from these instruments are statistically partitioned among the various plasma sheet ion species, using the empirical density ratios found by *Young et al.* [1982] (hereafter Y82). The resulting boundary density or flux (n_b or Φ_b) of ring current species α is thus a function of the LANL quantities and the Y82 density ratios,

$$n_{b,\alpha} = \frac{n_{LANL}\varsigma_{Y82,\alpha}}{\sum_{\beta}\varsigma_{Y82,\beta}\sqrt{m_{H^+}/m_\beta}} \qquad \Phi_{b,\alpha} = \frac{\Phi_{LANL}\varsigma_{Y82,\alpha}}{\sum_{\beta}\varsigma_{Y82,\beta}} \tag{2}$$

where $\varsigma_\alpha = n_\alpha / n_{H^+}$. This method not only divides the LANL

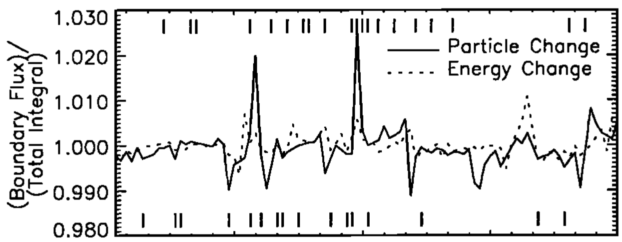

Figure 1. Numerical accuracy of the technique in terms of the change in total particles and energy, presented here as the ratio of the change calculated by summing the fluxes out the boundaries to the change calculated by differencing integrations over the entire simulation domain. The ticks across the top and bottom indicate when ΔN/Δt or ΔE/Δt, respectively, changes sign (the methods simultaneously change sign).

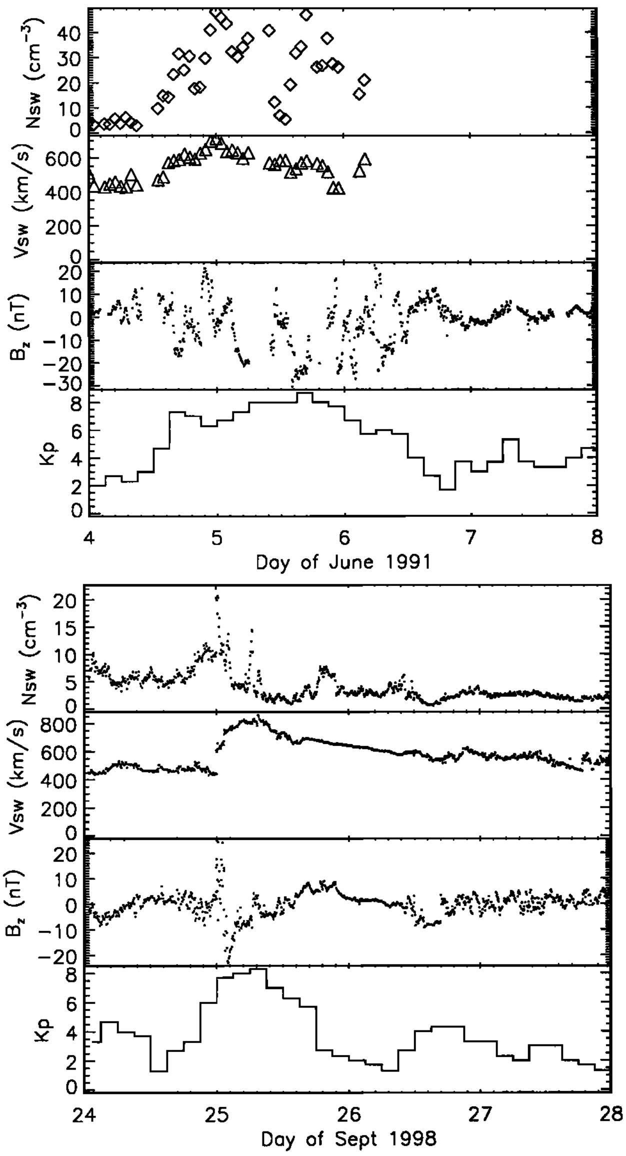

Figure 2. Solar wind density (top row) and velocity (second row), the z component of the IMF (third row), and Kp index (bottom row) for June 4-7, 1991 (left column) and September 24-27, 1998 (right column). The solar wind and IMF data are taken from IMP-8 and ACE for the two storms, respectively.

measurements between the two species according to the Y82 formulation, but also preserves the fluxes measured by MPA and SOPA whether density or flux is used. Note that a Maxwellian spectra is assumed in the flux partitioning equation, which may not be exact but will only cause a small deviation. For the two storms, the O^+ content predicted by Y82 reaches 70% for June 1991 and 40% for September 1998. The O^+ contribution to the total ring current energy generally follows this value with some recovery timescale. The model is run separately for O^+ and H^+, starting with an initially quiet distribution for each case and running for nearly four days.

The calculated *Dst* is plotted against the measured *Dst* (and its ring current component Dst^*, subtracting out diamagnetic effects [*Dessler and Parker*, 1959] and magnetopause currents [*Burton et al.*, 1975]) for both storms in Figure 3. The model results are found using the Dessler-Parker Sckopke relationship [*Dessler and Parker*, 1959; *Sckopke*, 1966], which calculates *Dst* from the total energy in the ring current. In general, the ring current evolution during the storms is well captured by the model, especially the magnitude of the minimum and the recovery rate. Missing features are most often the result of data gaps in the selected boundary condition.

Figure 4 shows the total net energy growth rates during the storms. It is clear that convective drift is both the largest source and loss of particles and energy during the main phases of the storms. For both events, dayside losses are significantly larger than charge exchange losses until some time into the late phase of the storm recovery. Atmospheric precipitation, collisional decay, and the net change due to energy drift are relatively minor terms in the total loss scenario for these two storms. Also shown in Figure 4 are the Shue et al. [1998] formula predictions for the subsolar magnetopause locations. Note that during the 1991 storm, the magnetopause crosses the simulation boundary several times for extended periods, but during the 1998 storm, it crosses only once for less than an hour. While loss enhancements coincide with these boundary crossings, it is the convective drift pushing the material across the compressed dayside boundary that accounts for the bulk of this loss.

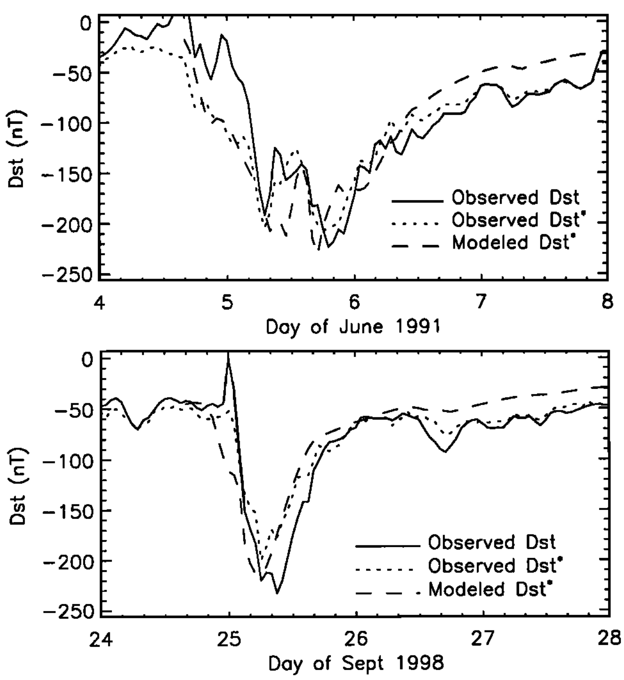

Figure 3. Observed *Dst*, Dst^*, and calculated Dst^*.

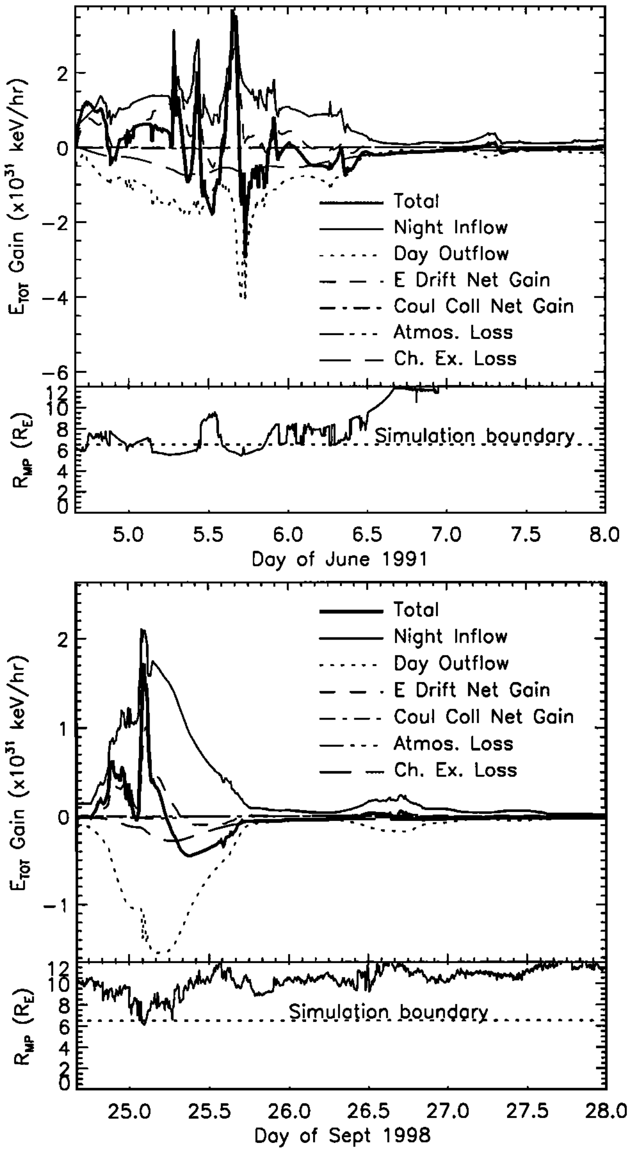

Figure 4. Time sequence of the energy source and loss mechanisms (first and third panels) and the subsolar magnetopause location (second and fourth panels) for the two storms (upper and lower pairs). Inflow and outflow are from the second and third terms in (1), *E* drift is from the fourth term in (1), Coul. Coll. are inelastic losses with particles, Atmos. Loss includes all pitch angle scattering and drift terms into the loss cone, and Ch. Ex. is charge exchange with neutral hydrogen. R_{MP} is calculated from the model of *Shue et al.* [1998].

The dominance of dayside drift loss is highlighted in Figure 5, which shows the ratio of the dayside outflow energy loss rate to the charge exchange energy loss rate. During the rapid early decay phases of both storms, this ratio always exceeds unity. For June 1991, the ratio rarely exceeds five, while for September 1998 the ratio exceeds 10 during the main phase. The spikes in the ratio are at times when the magnetopause encroached on the simulation domain, causing extra loss out the dayside. However, outflow is dominant with or without these

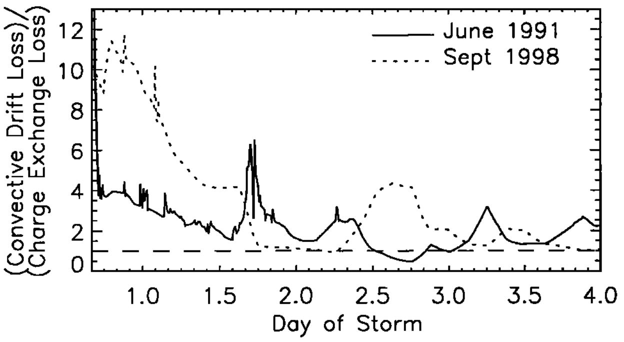

Figure 5. Ratio of the energy drift loss out the dayside to the energy charge exchange loss for H^+ (top panel), O^+ (middle panel), and the total ring current (bottom panel) for both storms. A dashed reference line at 1.0 is also drawn.

spikes, indicating that the strength of convection is the main driver of the outflow rate. The difference between the two storms indicates that charge exchange is more significant during solar maximum, but still not the dominant loss process. Not until the late phase of the storm recovery, when convection has decreased, does this ratio reach unity.

The model results show that drift losses out the dayside magnetopause are the major loss mechanism of ring current ions during the early phase of both storms. Charge exchange is always a contributor to the decay rate, and the agreement between the simulated and the observed *Dst* would certainly not have been reproduced without this process. However, it is not the primary method of removing ring current ions from the inner magnetosphere. Charge exchange begins to dominate later in the storm, once the plasma sheet injection has subsided and the non-trapped particles have convected through the inner magnetosphere. This means that the bulk of the *Dst* minimum is not due to the symmetric ring current, but rather due to plasma sheet material passing once by on the dusk side of the Earth and escaping out the dayside without making a complete revolution around the Earth. Therefore, these results quantitatively and more rigorously substantiate the idea proposed by *Takahashi et al.* [1990] that the two-phase decay is dominated by outflow during the early stage followed by inner magnetospheric losses during the late stage.

Acknowledgments. This work was supported by NASA grant NAG5-4771 and NSF grants ATM-9711381 and ATM-9800830. The authors would like to thank Joe Borovsky for useful comments and input.

References

Belian, R. D., G. R. Gisler, T. Cayton, and R. Christensen, High-Z energetic particles at geosynchronous orbit during the great solar proton event series of October 1989, *J. Geophys. Res.*, *97*, 16,897, 1992.

Burton, R. K., R. L. McPherron, and C. T. Russell, An empirical relationship between interplanetary conditions and *Dst*, *J. Geophys. Res.*, *80*, 4204, 1975.

Chen, M. W., J. L. Roeder, J. F. Fennell, L. R. Lyons, and M. Schulz, Simulations of ring current proton pitch angle distributions, *J. Geophys. Res.*, *103*, 165, 1998.

Chen, M. W., J. L. Roeder, J. F. Fennell, L. R. Lyons, R. L. Lambour, and M. Schulz, Proton ring current pitch angle distributions: Comparison of simulations with CRRES observations, *J. Geophys. Res.*, *104*, 17,379, 1999.

Daglis, I. A., The role of magnetosphere-ionosphere coupling in magnetic storm dynamics, in *Magnetic Storms, Geophys. Monogr. Ser.*, vol. 98, edited by B. T. Tsurutani, W. D. Gonzalez, Y. Kamide, and J. K. Arballo, p. 107, AGU, Washington, DC, 1997.

Dessler, A. J., and E. N. Parker, Hydromagnetic theory of geomagnetic storms, *J. Geophys. Res.*, *64*, 2239, 1959.

Fok, M.-C., T. E. Moore, J. U. Kozyra, G. C. Ho, and D. C. Hamilton, Three-dimensional ring current decay model, *J. Geophys. Res.*, *100*, 9619, 1995.

Hamilton, D. C., G. Gloeckler, F. M. Ipavich, W. Studemann, B. Wilken, and G. Kremser, Ring current development during the great magnetic storm of February 1986, *J. Geophys. Res.*, *93*, 14,343, 1988.

Jordanova, V. K., L. M. Kistler, J. U. Kozyra, G. V. Khazanov, and A. F. Nagy, Collisional losses of ring current ions, *J. Geophys. Res.*, *101*, 111, 1996.

Jordanova, V. K., C. J. Farrugia, L. Janoo, J. M. Quinn, R. B. Torbert, K. W. Ogilvie, R. P. Lepping, J. T. Steinberg, D. J. McComas, and R. D. Belian, October 1995 magnetic cloud and accompanying storm activity: Ring current evolution, *J. Geophys. Res.*, *103*, 79, 1998.

Kozyra, J. U., M.-C. Fok, E. R. Sanchez, D. S. Evans, D. C. Hamilton, and A. F. Nagy, The role of precipitation losses in producing the rapid early recovery phase of the Great Magnetic Storm of February 1986, *J. Geophys. Res.*, *103*, 6801, 1998.

Liemohn, M. W., G. V. Khazanov, and J. U. Kozyra, Banded electron structure formation in the inner magnetosphere, *Geophys. Res. Lett.*, *25*, 877, 1998.

McComas, D. J., S. J. Bame, B. L. Barraclough, J. R. Donart, R. C. Elphic, J. T. Gosling, M. B. Moldwin, K. R. Moore, and M. F. Thomsen, Magnetospheric plasma analyzer: initial three-spacecraft observations from geosynchronous orbit, *J. Geophys. Res.*, *98*, 13,453, 1993.

Sckopke, N., A general relation between the energy of trapped particles and the disturbance field near the Earth, *J. Geophys. Res.*, *71*, 3125, 1966.

Shue, J.-H., P. Song, C. T. Russell, J. T. Steinberg, J. K. Chao, G. Zastenker, O. L. Vaisberg, S. Kokubun, H. J. Singer, T. R. Detman, and H. Kawano, Magnetopause location under extreme solar wind conditions, *J. Geophys. Res.*, *103*, 17,691, 1998.

Takahashi, S., T. Iyemori, and M. Takeda, A simulation of the stormtime ring current, *Planet. Space Sci.*, *38*, 1133, 1990.

Young, D. T., H. Balsiger, and J. Geiss, Correlations of magnetospheric ion composition with geomagnetic and solar activity, *J. Geophys. Res.*, *87*, 9077, 1982.

J. U. Kozyra and M. W. Liemohn, Space Physics Research Laboratory, University of Michigan, 2455 Hayward St., Ann Arbor, MI 48109. (email: liemohn@umich.edu; jukozyra@umich.edu)

V. K. Jordanova, Space Science Center, University of New Hampshire, Durham, NH 03824. (email: vania.jordanova@unh.edu)

G. V. Khazanov, Geophysical Institute, University of Alaska Fairbanks, Fairbanks, AK 99775. (email: khazanov@gi.alaska.edu)

T. E. Cayton and M. F. Thomsen Los Alamos National Laboratory, Los Alamos, NM 87545. (email: mthomsen@lanl.gov; tcayton@lanl.gov)

(Received June 21, 1999; accepted July 29, 1999.)